Balancing Biomechanics and Preference in Assistive Device Tuning via Metric-Regularized Optimization

Dabin K. Choe*, Digby Chappell*, Ashlyn J. Aiello, Christina Lee, Kimberly Ang, Louis N. Awad, and Conor J. Walsh†

***Abstract*— *Objective:* Gait-assistive technology has the potential to benefit millions, but adoption is limited by challenges in tuning assistance to simultaneously provide biomechanical benefits and satisfy patient and clinician preference. In this study, we quantify the dissonance between these outcomes, inspect its sources, and propose methods to address it. *Methods:* We collected biomechanics and preference data from nine individuals post-stroke using a plantarflexion neuroprosthesis, and 96 corresponding preference datasets from 36 clinicians. We inspected the biomechanics and preference modeled outcomes occurring when either outcome was optimized in isolation. Then, we used weighted sums of biomechanical principal components to identify determinants of preference for patients and clinicians, and inspected their anatomical locations. Finally, we extended this weighting method to biomechanical metrics, and developed a method of balancing preference with multiple metric outcomes. *Results:* We found that maximizing modeled preference or biomechanics produced poor modeled outcomes in the other domain. Patient and clinician preference could be strongly approximated with fewer than five extracted biomechanical determinants, though heterogeneity of determinants across individuals was high. Our metric-preference balanced method of tuning assistance significantly improved preference outcomes compared to metric-optimal assistance and prevented negative biomechanical outcomes for individualized sets of both one and ten metrics. *Conclusion:* This work demonstrates the importance of both biomechanics and preference in gait-assistive device tuning, highlights the individualized nature of the biomechanical determinants of preference, and demonstrates, via offline modeling, that balancing biomechanics and preference is possible. *Significance:* This work highlights the necessity and feasibility of balanced tuning in gait-assistive devices.**

***Index Terms*— Assistive and Rehabilitative Technology, Personalized Assistance, Gait Biomechanics, User Preference**

Submitted on XXXX. This work was supported in part by the National Institutes of Health (NIH) Blueprint for Neuroscience Research, and by the following NIH institutes: the National Institute of Child Health and Human Development (NICHD) and the National Institute of Neurological Disorders and Stroke (NINDS/BRAIN) through grant U54EB033664, subproject #15922. It was also supported in part by the Massachusetts Technology Collaborative under Grant 268439-5121224 and the Raj Bhattacharyya and Samantha Heller Assistive Technology Initiative Fund.

D. K. Choe, C. Lee, and C. J. Walsh are with the Harvard John A. Paulson School of Engineering and Applied Sciences, Harvard University, Boston MA, 02134, USA. (†e-mail: walsh@seas.harvard.edu).

D. Chappell is with the Department of Engineering Science, University of Oxford, Oxford, OX1 3PJ.

A. J. Aiello, K. Ang, and L. N. Awad are with the Sargent College of Health and Rehabilitation Sciences, Boston University, Boston MA, 02215, USA.

*D. K. Choe and D. Chappell contributed equally to this work.

I. Introduction

WEARABLE gait assistive and rehabilitative technologies, such as robotic exosuits, exoskeletons, and neuroprostheses, have emerged as promising tools to restore mobility across diverse populations [1], [2], [3], [4], [5], [6]. These devices provide assistance through a number of mechanisms [7], [8], offering immediate gait improvement [6] as well as long-term rehabilitative benefits [9].

Despite their demonstrated benefits to gait biomechanics in research studies, wearable devices continue to face barriers to widespread adoption, reflected in low prescription [10] and high abandonment rates [11], [12]. A key challenge lies in providing effective assistance by devices to match individual needs. Furthermore, improper tuning of devices can adversely impact biomechanics, leading to significantly worse gait outcomes [6]. For assistive and rehabilitative devices to achieve widespread clinical adoption, it is important to balance biomechanical efficacy with patient and clinician perceptions of assistance, comfort, and safety [13]. Traditional approaches such as expert manual tuning and human-in-the-loop optimization have mostly focused on maximizing biomechanical outcomes or energy efficiency [14], [15], [16], [17], yet these approaches often neglect user perception and preference, which are factors crucial to patient adherence, clinician prescription, and ultimately long-term device acceptance [13], [18], [19]. On the other hand, recent studies have demonstrated the utility of using user preference as an objective for tuning assistive devices, achieving promising results across a variety of devices, including rigid exoskeletons [20], [21], [22], prostheses [23], and robotic emulators [24]. However, to date, preference-based tuning methods have been conducted independently of biomechanical outcomes, meaning there is no guarantee of delivering biomechanical benefits to the user. Given the complexities of human-device interaction and the fact that both biomechanics and preference are influencing factors of assistive device adoption, there is a clear need to investigate the outcomes from tuning these factors separately.

At present, the biomechanical outcomes associated with preference-based tuning are not well understood, along with the biomechanical determinants of perception [22], [25]. Prior studies have highlighted divergence between user preference and widely used biomechanics-based performance metrics in terms of energy expenditure when adopting prescribed

gait patterns [26], energy storage and return when tuning joint stiffness in lower limb prostheses [27], and metabolic efficiency when tuning exoskeletons [28], [29] and lower limb prostheses [30]. In order to balance these divergent tuning paradigms, there is a need to investigate the outcomes associated with tuning for biomechanics or preference, identify potential conflicts between them, and develop strategies that align these potentially dissonant objectives for improved device efficacy and acceptance by both clinicians and patients.

Beyond differences between biomechanical metrics and user preference, another crucial, yet often overlooked, factor is the potential discrepancy between patient and clinician perceptions of device efficacy. While clinicians rely primarily on visual assessments of gait, patients rely on their direct experience, creating potentially differing perceptions of comfort, assistance and safety. Despite inherent synergy between clinicians and patients in acceptance of assistive and rehabilitative devices, where acceptance by one group influences acceptance by the other [13], these perceptual differences may complicate tuning decisions and warrants further investigation. For example, in the case of prosthetic ankle tuning, prosthetists and patients preferred different stiffness values [31]. To begin addressing the challenge of accommodating conflicting preferences, resultant preferences and their associated biomechanical determinants for both clinicians and patients should be examined.

Tuning parameters to satisfy the preferences of multiple stakeholders (clinicians and patients) while achieving desired biomechanical outcomes is especially challenging in populations with neurological gait impairments. This encompasses a vast number of individuals, with causes such as stroke, spinal cord injury, and traumatic brain injury that affect hundreds of millions of people worldwide [32], [33], [34], [35]. This additional complexity in assisting individuals with neurological gait impairment arises from inherent gait pattern heterogeneity [36], [37], [38], varying chronicity [39], [40], and individual-specific functional goals [41], [42], which together necessitate high levels of personalization to provide effective assistance. Furthermore, safety, comfort, and therapeutic efficacy often present competing priorities for populations with neurological gait impairments, as greater levels of assistance may come at the cost of increased discomfort or perceived safety concerns, leading to lower adherence rates [43], [44]. The emphasis on individualization, paired with these competing considerations may lead to conflicts and reduced adherence. Given that successful gait neuro-rehabilitation is predicated on high-dosage, consistent device usage [45], [46], understanding how biomechanical performance, clinician perception, and patient perception interact becomes essential to achieving both clinical efficacy and widespread acceptance. The majority of existing preference-based tuning studies have predominantly focused on populations without neurological impairment or devices with simple tuning parameter spaces [29], [47], [48], [49], so it remains unclear how these findings may translate to clinical populations and devices with more complex multi-dimensional parameter spaces. Ultimately, for gait assistive technology to benefit clinical populations with neurological gait impairments, there is a pressing need to understand the biomechanical determinants of preference, and explore the potential of preference-based tuning specifically for these populations. Addressing these challenges is essential to the advancement of robotic assistive technologies, enabling them to transition effectively from laboratory to clinical use.

In this work, we study the relationship between biomechanical outcomes and patient and clinician preference outcomes, using lower-limb neuroprosthesis parameter tuning as a model of how these competing objectives could be balanced. We first model biomechanical and preference outcomes in response to gait assistance. We then quantify the level of dissonance associated with tuning assistance to maximize either modeled biomechanics or preference outcomes in isolation. To understand this further, we present a method of approximating modeled preference with a weighted sum of normalized biomechanical models, and inspect key differences in how these biomechanical variables are prioritized when approximating patient and clinician preference. Finally, we propose a balanced method of tuning assistance using metric-regularized preference maximization, which optimizes modeled preference within assistance parameter regions that guarantee positive outcomes of modeled biomechanical point metrics, and perform offline evaluation of this method on our collected dataset against isolated optimization of modeled biomechanical or preference outcomes.

II. Methods

In this section, we first describe the collection of patient spatiotemporal, kinematic, and kinetic gait data (henceforth referred to as biomechanical data), the collection of patient and clinician preference data, and the plantarflexion neuroprosthesis used to deliver gait assistance. Then, we outline methods used to create models of changes to each participant's biomechanics and preference induced by delivered assistance, which we use to compare optimal outcomes in each domain (preference and biomechanics). Then, we present a method of approximating the modeled response of a participant in one domain by modeled responses in another domain, which we use to quantify biomechanical correlates and determinants of preference. Finally, we present a method of using biomechanical metric determinants of preference to penalize assistance parameter tuning, resulting in metric-regularized preference maximization.

A. Study overview

Functional electrical stimulation (FES) was delivered to plantarflexor and dorsiflexor muscles of the paretic leg of participants with chronic post-stroke hemiparesis (see Fig. 1 **A**). The assistance parameters $\boldsymbol{a} = [\tau, I]^T$ varied were plantarflexion sitmulation onset timing, τ, and amplitude, I (see Fig. 1 **B** and **C**), while dorsiflexor stimulation was held fixed in order to maintain safe toe clearance during walking. The biomechanical outcomes considered in this study were extracted outcomes via multivariate functional principal component analysis (MFPCA), and metric outcomes covering a range of kinetic, kinematic, and spatiotemporal metrics that are commonly used in biomechanics studies (see Supplementary Methods and Fig. 1 **E**). Patient preference was collected in parallel with biomechanical data collection via a series of two-interval forced choice (2IFC) questions separately comparing the relative perceived safety,

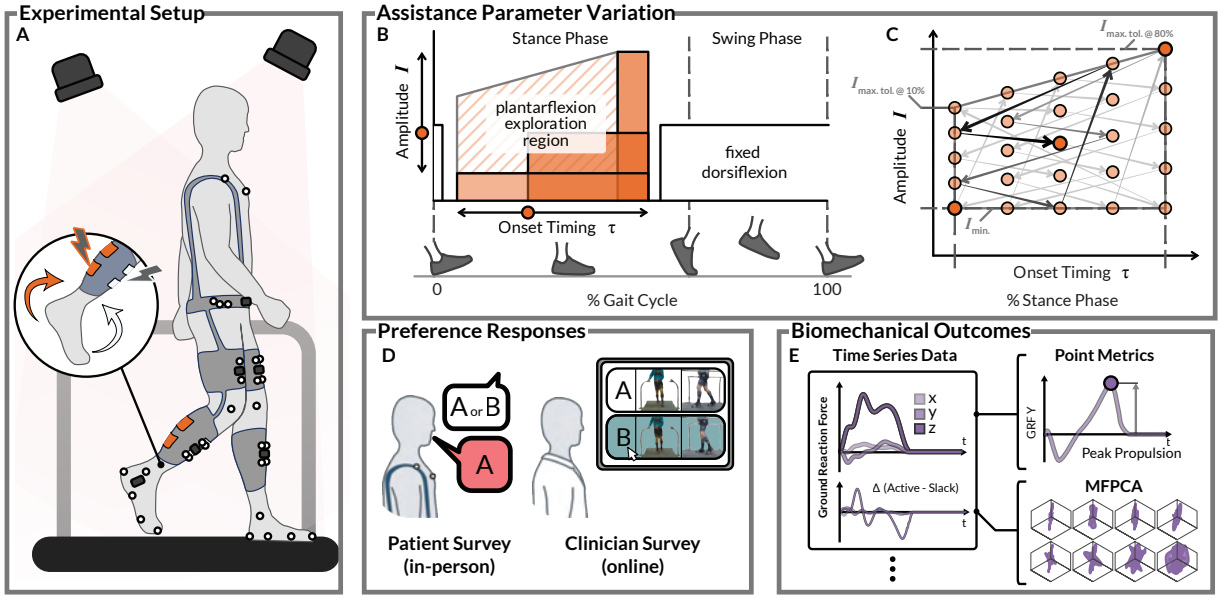

Fig. 1: Experimental setup extracting biomechanical and preference responses to trial sets of assistance parameter values. (**A**) Participants trialed stimulation profiles during fixed-speed treadmill walking, while ground reaction force and motion capture data were collected. (**B**) Plantarflexor stimulation onset timing and amplitude were varied while plantarflexor stimulation offset and dorsiflexor stimulation were fixed. (**C**) 25 stimulation profiles were tested. Profiles were sampled systematically such that perceptual difference between subsequent profiles was maximized and no overall trend was present in the full sequence of amplitudes and onset timings. (**D**) Patient preference was collected in-session via a series of two-interval forced choice questions comparing subsequent stimulation profiles. Clinician preference was collected via a series of two-alternative forced choice questions comparing patient videos. (**E**) Biomechanical time-series data were collected during active (with stimulation) and slack (no stimulation) walking. Point-based metrics were extracted from both conditions, and multivariate functional principal component analysis (MFPCA) was performed on the difference between active and slack time-series data to capture changes due to assistance.

comfort, and assistance of sequential periods of assistance, separated by unassisted washout periods (see Fig. 1 **D** left). Clinician preference was obtained via a series of two-alternative forced choice (2AFC) questions with identical wording to patient questions, in response to frontal and paretic-side sagittal plane videos of each patient walking with assistance, showing sequential assistance profiles side-by-side in the order they were experienced by the patient (see Fig. 1 **D** right).

1) Patient Data Collection: Patients performed five treadmill walking bouts at 70% of their self-selected comfortable walking speed, each consisting of alternating 30-second duration no-assistance and assistance trials for six minutes. Participants were exposed to a total of 25 assistance profiles; six different assistance profiles during each walking bout, with the first profile matching the last profile from the previous bout. All biomechanics data were collected at 200 Hz using 18 optical motion capture cameras (Qualisys AB; Sweden) and two 6 degree of freedom (DOF) force plates mounted beneath each belt of a split-belt treadmill (Bertec Corp.; USA). Kinetic and kinematic joint biomechanical data were processed with inverse dynamics using a commercial motion analysis software (Visual3D, C-Motion Inc.; USA) and were filtered using a fourth-order Butterworth low-pass filter with a 10 Hz cutoff frequency. Changes in gait biomechanics were computed relative to the no-assistance condition immediately preceding an assistance condition to account for participant adaptation and fatigue.

2) Functional Electrical Stimulation System: The lower limb neuroprosthesis presented in [6] was used to deliver unilateral functional electrical stimulation (FES) assistance to the muscle belly of the tibialis anterior for dorsiflexion, and the gastrocnemius for plantarflexion. Stimulation frequency and pulse duration were held at 40 Hz and 400 μs, respectively, and amplitude was kept constant within a pulse train.

3) Stimulation Parameter Sampling and Exploration Bounds: The exploration region for onset timing τ of plantarflexor stimulation was constrained between $\tau_{\min} = 10\%$ and $\tau_{\max} = 80\%$ of paretic stance phase to ensure that generated ankle torque contributed to forward movement of the body. To avoid inducing co-contraction, plantarflexor stimulation was terminated at 85% of the estimated paretic stance phase.

To form an exploration region for plantarflexor stimulation amplitude, each participant's motor-point amplitude, I_{motor}, and the maximum tolerable amplitude at both 10% ($I_{\text{max. tol. @10\%}}$) and 80% ($I_{\text{max. tol. @80\%}}$) onset timing was found. During trials, amplitude was varied between a linear upper bound, scaled with onset timing between $I_{\text{max. tol. @10\%}}$ and $I_{\text{max. tol. @80\%}}$, and a lower bound $I_{\text{min.}}$. of:

$$I_{\text{min.}} = I_{\text{motor}} + 0.25(I_{\text{max. tol. @80\%}} - I_{\text{motor}}). \quad (1)$$

25 assistance profiles were sampled from the trapezoidal exploration region (see Fig. 1 **C**) using systematic sampling with a randomized starting point with two criteria. First, the parameter space distance between sequential samples should be maximal, to ensure that the perceptual difference between samples was safely above just noticeable difference for preference responses. Second, the sampled values of each parameter should be a time-stationary signal, to avoid biasing a participant's preference over the course of the session. After flattening the 5×5 grid of parameter values, sampling step sizes in the range $[1, 25)$ were

tested. A step size of 9 was found to produce a statistically time-stationary sequence ($p < 0.001$ amplitude, $p < 0.05$ onset timing, Augmented Dickey-Fuller test) with an average subsequent sample difference of 1.625 indices in stimulation amplitude and 2.208 indices in onset timing.

For all trials, dorsiflexor stimulation was delivered from 95% of the estimated paretic stance phase to 90% of the estimated non-paretic stance phase, as in our previous work [6].

B. Modeling and Comparing Preference and Biomechanics

To estimate optimal assistance parameter values and quantitatively compare preference and biomechanical outcomes, Gaussian process regression was used to model each outcome as a function of assistance parameter values $\boldsymbol{a}$. For biomechanical outcomes, this meant forming models of principal component scores $Y(\boldsymbol{a})$ and metric outcomes $M(\boldsymbol{a})$ from datasets of computed principal component scores $\mathcal{D}_y = [y_1, \ldots, y_{25}]^T$ and metric outcomes $\mathcal{D}_m = [m_1, \ldots, m_{25}]^T$, respectively.

For preference, this meant forming models of patient preference $P(\boldsymbol{a})$ and clinician preference $C(\boldsymbol{a})$ from datasets of pairwise comparisons between the 25 assistance profiles $\mathcal{D}_p = [p_1, \ldots, p_{25}]^T$, and $\mathcal{D}_c = [c_1, \ldots, c_{25}]^T$, respectively, where p_i and c_i are binary indicators of whether profile i was preferred to profile $i+1$. In total, three preference models were created per patient ($P_s(\boldsymbol{a})$, $P_c(\boldsymbol{a})$, and $P_a(\boldsymbol{a})$)) and clinician ($C_s(\boldsymbol{a})$, $C_c(\boldsymbol{a})$, and $C_a(\boldsymbol{a})$); one each for safety, comfort, and assistance.

1) Computing Biomechanical Responses to Assistance: The following biomechanical variables were recorded from the paretic leg of each participant during walking trials using motion capture: ground reaction force **GRF**, center of pressure **COP**, foot orientation $\boldsymbol{\theta}_{\text{foot}}$, foot position $\boldsymbol{x}_{\text{foot}}$, ankle angle $\boldsymbol{q}_{\text{ankle}}$, ankle torque $\boldsymbol{\tau}_{\text{ankle}}$, knee angle $\boldsymbol{q}_{\text{knee}}$, knee torque $\boldsymbol{\tau}_{\text{knee}}$, hip angle $\boldsymbol{q}_{\text{hip}}$, hip torque $\boldsymbol{\tau}_{\text{hip}}$, trailing limb angle TLA (extracted as in [50]), pelvis orientation $\boldsymbol{\theta}_{\text{pelvis}}$, and pelvis position $\boldsymbol{x}_{\text{pelvis}}$. The following spatiotemporal variables were also computed: stance phase duration, T_{stance}, swing phase duration, T_{swing}, and stride duration, $T = T_{\text{stance}} + T_{\text{swing}}$.

We used MFPCA to decompose the stride-normalized time series data from a given biomechanical variable $\boldsymbol{b}(t), t \in [0, T]^T$ across a stride of duration T (for example, foot position) to a summation of a mean function $\bar{\boldsymbol{b}}(t)$ and a series of K multivariate functional principal components $\beta_k(t)$ weighted by corresponding principal component (PC) scores $y^{(k)}$:

$$\boldsymbol{b}(t) = \bar{\boldsymbol{b}}(t) + \sum_{k=1}^{K} y^{(k)} \beta_k(t), \tag{2}$$

For the mean stride time series data from each assistance profile, the corresponding PC score was calculated (see Supplementary Methods for details) to form a dataset of principal component responses D_y for each biomechanical variable and principle component. MFPCA was used to extract a total of $N_y = 96$ principal component (PC) responses; $K = 8$ PCs extracted from each of 12 multivariate biomechanical variables (excluding TLA), which was sufficient to capture a minimum of 80% variance for each biomechanical variable for every patient.

Concurrently, $N_m = 20$ biomechanical point metrics found in literature (see Supplementary Table S10) were also calculated: propulsive impulse, mean vertical GRF, anterior-posterior COP excursion, medio-lateral COP excursion, foot-to-floor angle at initial contact, maximum lateral circumduction, peak ankle torque, peak plantarflexion angle, ankle inversion at initial contact, peak knee extension torque, peak knee extension, peak hip flexion torque, peak trailing limb angle, peak hip abduction, pelvis angle excursion, hip hiking, stride length, stance time, stance-swing ratio, and stride time variability. Each biomechanical point metric was computed from the mean stride time series data from each assistance profile.

See Supplementary Methods for details of extracting principal component responses and for point metric definitions.

2) Modeling Changes in Biomechanical Metrics: To model changes in gait biomechanics in response to assistance parameter values relative to unassisted walking, Gaussian process regression was used, following [51], where the regression function to be modeled is a multivariate Gaussian. For each patient, this modeling was performed for the N_y principal component responses extracted from biomechanical variables, forming $Y_1(\boldsymbol{a}), \ldots, Y_{N_y}(\boldsymbol{a})$ models, and for the N_m biomechanical point metric responses, forming $M_1(\boldsymbol{a}), \ldots, M_{N_m}(\boldsymbol{a})$ models. See Supplementary Methods Gaussian process fitting details.

3) Modeling Patient and Clinician Preference: From the collected preference datasets, models were created of each participant's latent utility function; the underlying true value in terms of preference of an assistance profile. The preference learning framework presented in [52] was used for this, in which a multivariate Gaussian prior was defined across all latent utilities, and uncertainty was present in latent utilities, modeled by internal white noise. From this, the posterior distribution was computed via Bayes' rule (see Supplementary Methods). Mann-Kendall tests were used to detect the monotonic trend in a corrupted preference data that occurred when a participant exhibited an order-based bias (for example, consistently favoring the first option in each pairwise comparison). Datasets with significant trends were discarded, resulting in $N_{P,s} = 9$, $N_{P,c} = 9$, and $N_{P,a} = 7$ patient models and $N_{C,s} = 90$, $N_{C,c} = 92$, and $N_{C,a} = 90$ clinician models for safety, comfort, and assistance preferences respectively.

4) Comparing Models of Biomechanics and Preference: To compare optimal modeled outcomes across each domain, biomechanical metric-optimal $\hat{M}$ outcomes and patient $\hat{P}$ and clinician $\hat{C}$ preference-optimal outcomes, and their corresponding assistance parameter values were extracted. For example, the assistance parameter values that maximize a modeled clinician's preference response can be extracted (with similar formulations for metric and patient optimal assistance parameter values):

$$\hat{\boldsymbol{a}}_C = \text{argmax}(C(\boldsymbol{a})). \tag{3}$$

Following this, the corresponding patient, clinician, and biomechanical responses to a given set of optimal assistance parameter values can be estimated (see Fig. 2 **A**). For example, the modeled patient preference response to assistance parameter values that maximize modeled clinician preference can be estimated:

$$P_{\hat{C}} = P(\hat{\boldsymbol{a}}_C). \tag{4}$$

To quantify agreement between pairs of models, we calculated the Spearman's rank correlation coefficient between modeled

responses at the 25 trialed parameter values.

To enable better comparison within and between modeled preference and metric-based outcomes, when reporting results we normalized outcomes. We normalized preference models to have zero mean and unit maximum value. Metric models were normalized such that zero corresponded to no change from unassisted walking, and to have unit maximum value.

C. Approximating and Balancing Preference and Biomechanical Models

1) Approximating Preference Models with Biomechanical Principal Component and Point Metric Models: To approximate preference models with biomechanical models, the mean functions of each Gaussian process were first scaled to have zero average response and unit standard deviation across each mean function. Approximate preference models, for example approximate patient preference P_{approx}, were computed as a linear weighted sum of N_a biomechanical principal component models $Y_1, \ldots, Y_{N_a}$:

$$P_{\text{approx}}(\boldsymbol{a}) = \sum_{j=1}^{N_a} w_j Y_j(\boldsymbol{a}). \tag{5}$$

The weight associated with each biomechanical principal component model was computed to minimize the mean function distance between the target preference model $P_{\text{target}}(\boldsymbol{a})$ and the approximate preference model $P_{\text{approx}}(\boldsymbol{a})$:

$$w_j = \text{argmin}(d(P_{\text{target}}(\boldsymbol{a}), P_{\text{approx}}(\boldsymbol{a}))). \tag{6}$$

Here, $d(\cdot,\cdot)$ is the average Euclidean distance between the mean functions of the Gaussian process models:

$$d(P_{\text{target}}(\boldsymbol{a}), P_{\text{approx}}(\boldsymbol{a})) = \frac{1}{A(\boldsymbol{a})} \int_{\boldsymbol{A}} ||P_{\text{target}}(\boldsymbol{a}) - P_{\text{approx}}(\boldsymbol{a})||_2 d\boldsymbol{a}, \tag{7}$$

where $A(\boldsymbol{a})$ is the area of the assistance parameter space that the two mean functions cover. This was repeated for preference approximations formed from models of biomechanical point metric responses $M_1, \ldots, M_{N_a}$. Due to the large number of biomechanical principal component and point metric responses, it was not computationally feasible to trial all combinations of responses in approximating preference. As a more tractable approach, biomechanical principal component models and biomechanical point metric models were sequentially added to the preference approximation. At each iteration, the addition of each possible remaining response model was trialed by recomputing the optimal weights, and the response model which resulted in the smallest approximation cost was kept. In experiments, we varied N_a to inspect the effects of changing the number of models on the resultant approximation.

2) Biomechanical Metric-Regularized Preference Maximization: To find assistance parameter values that maximize modeled preference while satisfying lower bounds on modeled biomechanical point metric outcomes, penalization was applied to assistance parameter regions that produced negative modeled metric outcomes. We selected the N_r biomechanical point metric models with the greatest preference approximation weighting magnitude in order to focus on biomechanical metrics that are determinants of preference. Penalization $g_j(\boldsymbol{a})$ from biomechanical point metric model j was applied to regions of negative modeled metric outcome, scaled by the approximation weight magnitude $|w_j|$, and normalized to the standard deviation σ_j of the measured metric responses during unassisted walking:

$$g_j(\boldsymbol{a}) = \frac{|w_j|}{\sigma_j} \min(M_j(\boldsymbol{a}), 0). \tag{8}$$

This gave a resultant response landscape, used to find optimal assistance parameter values, of:

$$P|_M(\boldsymbol{a}) = P(\boldsymbol{a}) + \alpha \sum_{j=1}^{N_r} g_j(\boldsymbol{a}), \tag{9}$$

where α is a penalization coefficient to be tuned to balance maximizing modeled preference outcomes with maintaining minimum modeled biomechanical point metric outcomes. Computing the maximum value of the resultant model produces a metric-regularized preference maxima $\hat{P}|_M$, with corresponding assistance parameter values $\hat{a}_{P|_M}$. Individual model responses to these parameter values are denoted $M_{\hat{P}|_M}$, etc. We varied the number of metric models used in regularization N_r and the global penalization coefficient α, and studied their effects on the resultant landscape and optimal outcomes.

D. Participants

$N_p = 9$ individuals with chronic post-stroke hemiparesis were recruited to this study (8 male/1 female, median [interquartile range (IQR)] age 52 [14] years; 9 [5] years since stroke). Patient characteristics are reported in Supplementary Table S8. Inclusion criteria consisted of a minimum age of 18 years, stroke chronicity greater than 6 months, the ability to walk independently with or without an assistive device for a minimum of 30 m, and a passive paretic ankle dorsiflexion range of motion to neutral (i.e. 90 degrees between foot and tibia). Participants were excluded if they had history of lower extremity joint replacement, metal implants beneath stimulation sites, and/or an inability to communicate with the study team. $N_c = 36$ clinicians with a median [IQR] experience of 6 [9] years working with individuals post-stroke; 1 [3] years working with functional electrical stimulation were recruited to this study (clinician characteristics are reported in Supplementary Table S9). All study procedures were approved by the Institutional Review Boards at Harvard University and Boston University, all participants provided written informed consent, and medical clearance was obtained from the primary healthcare providers of participants with post-stroke hemiparesis.

E. Statistical Analyses

Correlation of approximated preference response with target preference response data for patients and clinicians was statistically compared using a linear mixed effects model after Fisher transformation. The linear mixed effects model equation related transformed correlation to number of principal components (#PCs) and participant group (patient or clinician):

$$\text{Transformed Correlation} \sim \#\text{PCs} + \text{C(Group)} + \#\text{PCs} : \text{C(Group)}$$

To identify groups of principal components that appeared more or less than expected in an optimal set of models used to

approximate preference, two-sided proportions z-tests were used. To analyze the order in which models appeared in a set used to approximate preference, we computed normalized variable importance, where the rank score of groups of variables was normalized by their expected rank score (if models had been selected randomly), and one-sample Wilcoxon signed-rank tests were performed, with an expected value of 1.0. To test whether outcomes associated with patient-optimal assistance were significantly different from those associated with clinician-optimal assistance, two-sided Mann-Whitney U tests were used. For paired outcomes, e.g., preference outcomes in response to assistance parameter values that were metric-optimal versus metric-regularized preference-optimal, two-sample Wilcoxon signed-rank tests were used. Finally, to test whether metric outcomes were significantly greater than zero (indicating that negative metric outcomes had been avoided), one-sample Wilcoxon signed-rank tests were used. Where multiple statistical comparisons were made, Holm-Bonferroni corrections were applied to the p-values associated with each comparison.

III. Results

A. Dissonant preference and biomechanical metric responses with optimal assistance parameter values

To compare the outcomes of selecting assistance parameter values that optimize modeled preference and biomechanics, the modeled responses of 20 biomechanical point metrics were computed (see Supplementary Table S10, and Supplementary Methods for computation details). As seen in Fig. 2 and Supplementary Table S3, modeled patient and clinician preference-optimal assistance consistently led to poorer modeled metric outcomes than modeled biomechanical metric-optimal parameter values for kinematic, kinetic, and spatiotemporal metrics. As seen in Fig. 2 **B**, parameter values that maximized modeled patient and clinician preference produced median [IQR] increases in foot to floor angle at initial contact of 0.032 [0.044] radians, and 0.060 [0.079] radians, respectively, compared to a modeled biomechanical metric-optimal reduction in foot to floor angle of 0.132 [0.071] radians, corresponding to a significantly poorer outcome ($p < 0.05$ and $p < 0.01$ for modeled patient and clinician preference optimal, respectively, Mann-Whitney U test). Fig. 2 **C** shows similar results for change in propulsive impulse, with median [IQR] modeled biomechanical metric-optimal change in propulsive impulse of 0.068 [0.059] N.s/kg, significantly higher than modeled patient preference-optimal (-0.030 [0.101] N.s/kg, $p < 0.05$, Mann-Whitney U test), and clinician preference-optimal (0.000 [0.041] N.s/kg, $p < 0.001$, Mann-Whitey U test). For change in stance-swing ratio (see Fig. 2 **C**), the median [IQR] modeled biomechanical metric-optimal outcome was 0.201 [0.074], while modeled patient and clinician preference-optimal were 0.031 [0.127] and 0.057 [0.098], both significantly lower ($p < 0.05$ and $p < 0.01$, respectively, Mann-Whitney U test). Simultaneously, for both patients and clinicians, modeled biomechanical metric-optimal parameter values often led to worse than the average modeled preference outcome for each individual. This corresponds to respective median [IQR] normalized modeled patient and clinician preference outcomes of -0.176 [0.808] and -0.212 [0.674] for foot to floor angle-optimal parameter values (Fig. 2 **B**), -0.114 [0.473] and -0.102 [0.808] for propulsive impulse-optimal parameter values (Fig. 2 **C**), and -0.318 [0.59] and -0.051 [0.652] for stance-swing ratio-optimal parameter values (Fig. 2 **C**).

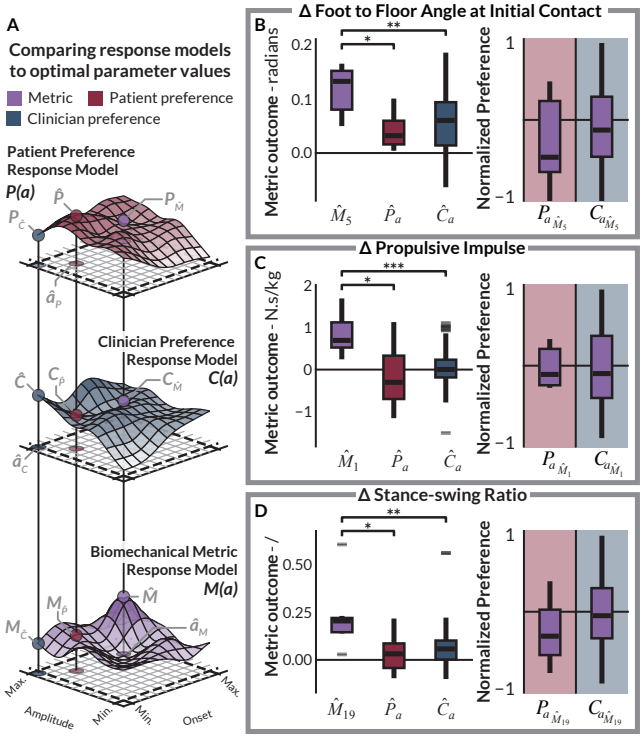

Fig. 2: Modeled biomechanical point metric and patient and clinician preference outcomes when selecting optimal assistance parameter values in isolation. (**A**) Extracting optimal modeled outcomes in terms of biomechanical metrics, clinician preference, and patient preference. (**B-D**) Modeled outcomes when tuning to maximize either modeled metric ($\hat{M}$) or modeled preference ($\hat{P}$ and $\hat{C}$) (normalized to have zero mean and unit maximum value) outcomes in isolation. Example metrics shown: M_5 foot to floor angle at initial contact (**B**), M_1 propulsive impulse (**C**), and M_{19} stance-swing ratio (**D**). Significance between metric-optimal and preference-optimal modeled biomechanical outcomes shown at $^{*}p < 0.05$, $^{**}p < 0.01$, and $^{***}p < 0.001$ levels, assessed using Mann-Whitney U-tests.

B. Identifying biomechanical determinants of preference

Models of preference and biomechanical principal components (see Fig. 3 **A-B**) were compared in terms of correlation coefficient magnitude. As seen in Fig. 3 **C**, individual biomechanical models were poorly correlated with preference, and very few individual models achieved even moderate ($0.4 < \rho < 0.6$) correlation with comfort preference. To approximate preference, a weighted linear sum of scaled biomechanical models was computed that minimized the distance between the mean functions of the preference and resultant approximated models. As seen in Fig. 3 **D**, strong correlation ($\rho > 0.8$) of the approximated model with modeled preference was observed within three to four PCs. Moreover, the biomechanical variables from which these top three PCs were extracted were highly varied across participants and the preferred factors of safety, comfort, and assistance (Supplementary Tables S5-S7).

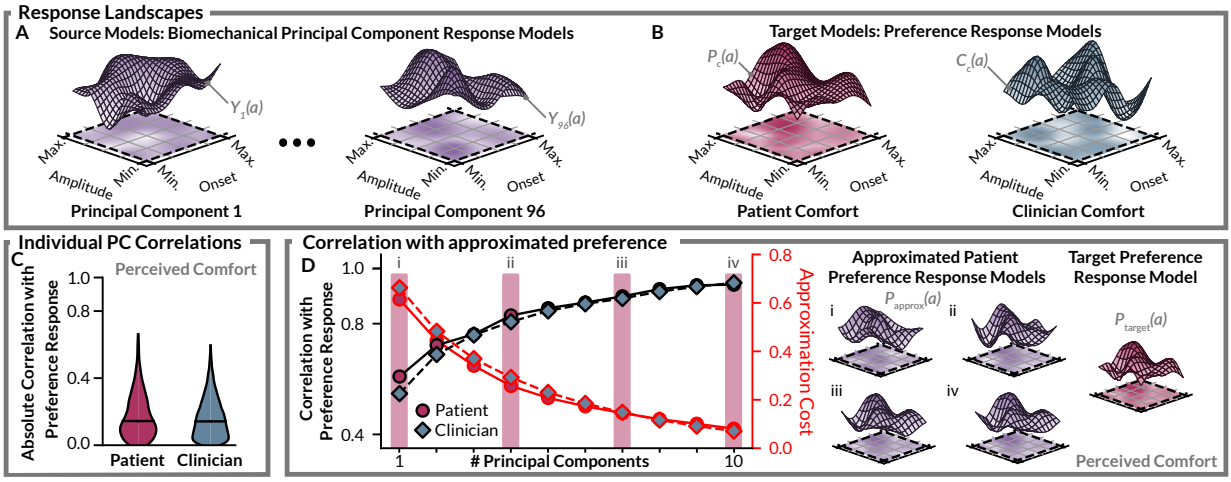

Fig. 3: Approximating patient and clinician preference models with extracted biomechanical principal component models. (**A-B**) Biomechanical principal component response models (**A**), and patient and clinician preference response models (**B**), modeled using Gaussian processes. (**C**) Correlation between biomechanical response models (N_y = 96 models per patient) and the comfort preference response models of patients ($N_{P,c}$ = 9 models) and clinicians ($N_{P,c}$ = 90 models). (**D**) Approximating patient and clinician preference models with a weighted sum of normalized biomechanical models to minimize Gaussian process mean function distance between the approximated and actual preference model.

We found that a significantly greater number of PCs were required to approximate models of clinician safety preference than patient safety preference ($p < 0.05$, linear mixed effects model), as seen in Fig. 4 **A**. To compare the relative importance of biomechanical variables in preference approximation, the rank-weighted approximation scores of groups of variable types were computed (see Fig. 4 **B-D**), as well as the prevalence of principal component models extracted from each biomechanical variable in the top three models used in preference approximation (see Supplementary Table S4). Considerable heterogeneity was observed in the biomechanical variables used for preference approximation, with no single variable type present in the majority of clinician and patient three-principal-component preference approximations. The only exception was hip torque, which appeared in four out of seven patient preference approximations of assistance; however, this was not statistically significant (see Supplementary Tables S4-S7). Knee torque, however, was present in preference approximations for a significantly low proportion of clinicians (see Supplementary Table S4) for all three perceived factors, prompting future investigation. As seen in Fig. 4 **B**, kinematic variables were significantly important in approximating modeled clinician safety preference, with a median [IQR] normalized importance value of 1.37 [0.43] ($p < 0.001$, Wilcoxon signed-rank test). The anatomical locations important in approximating modeled patient preference may be related to the preferred factor (safety, comfort, or assistance), hinted at by varied importance response for each preferred factor (see Fig. 4 **C**) and differences in the anatomical locations of the top three biomechanical variables in approximating any given patient's preferred factors (see Supplementary Tables S4-S7). However, these differences were not significant and a larger sample size would be needed to test this fully. For clinicians, this was not the case, with normalized importance of each anatomical location being approximately equal for safety, comfort, and assistance (see Fig. 4 **D**). This corroborates significantly high cross-correlations between each preferred factor for clinicians ($p < 0.001$ in all cases, one-sample t test after Fisher transformation, see Supplementary Fig. S1). In approximating modeled clinician preference, it was found that PCs extracted from the pelvis were significantly important in approximating safety, comfort, and assistance preference, with median [IQR] normalized importance values of 1.27 [1.47], 1.33 [1.23], and 1.33 [1.33] ($p < 0.01$, $p < 0.001$, $p < 0.01$; Wilcoxon signed-rank test), respectively, as seen in Fig. 4 **D**.

C. Balancing biomechanical outcomes and user preference

To evaluate our method of balancing modeled biomechanical and preference outcomes, we quantified the modeled outcomes of balanced profiles on the collected dataset of normalized biomechanical metric and preference models. As seen in Fig. 5 **A**, increasing the penalization coefficient ensured that selected parameter values do not produce negative modeled biomechanical outcomes, while increasing the number of metrics used for penalization captured more of the important biomechanical changes that influence preference, however increasing either reduced the positive proportion of the resultant cost landscape.

Fig. 5 **B** and **C** show normalized modeled preference outcomes when selecting assistance parameter values that maximize modeled metric outcomes ($\hat{M}$) in isolation and vice versa ($\hat{P}$), for the single most important metric (Fig. 5 **B**), and the 10 most important metrics (Fig. 5 **C**) in approximating preference. Also shown are the metric and preference outcomes of metric-regularized preference maximization with increasing penalization, when balancing a single metric response with preference response (Fig. 5 **B**), and when balancing 10 metric responses with preference response (Fig. 5 **C**). With a penalization coefficient of $k = 10^{0.5}$, balanced profiles yielded significantly better modeled preference outcomes than metric-optimal profiles, both for balancing one metric, where median modeled preference outcome increased from −0.40 to 1.00 ($p < 0.05$, two-sample Wilcoxon signed-rank test), and for balancing ten metrics, where median modeled preference outcome increased from −0.12 to 0.55 ($p < 0.001$, two-sample Wilcoxon signed-rank test). With the same penalization

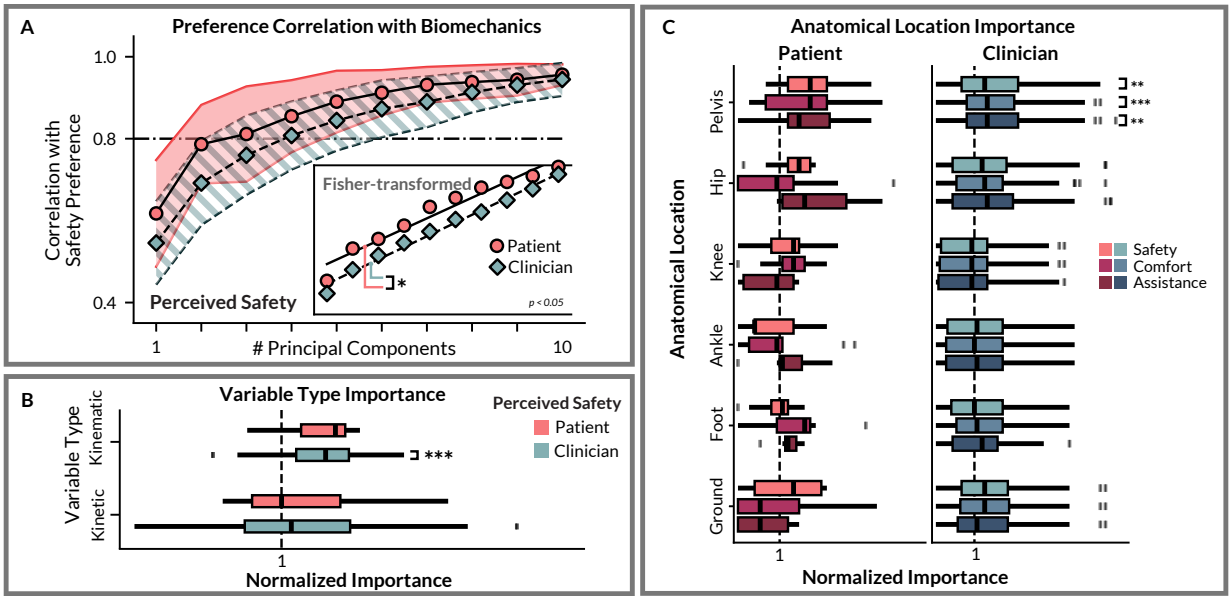

Fig. 4: Differences in principal component-based preference model approximation for patients and clinicians. (**A**) Correlation of approximated preference model with actual safety preference model for patients and clinicians, with Fisher-transformed correlation shown inset. Significance between patient and clinician correlation assessed using a linear mixed effects model, $^{*}p < 0.05$. (**B-C**) Rank score of biomechanical variables in approximating preference with 10 variables, grouped by variable type (**B**) and anatomical location (**C**), normalized by expected rank score if variables were selected randomly. Results significantly greater than a normalized importance of 1.0 assessed using Wilcoxon signed-rank tests, at levels $^{**}p < 0.01$, $^{***}p < 0.001$ after Holm-Bonferroni corrections for N=4 comparisons (**B**), and N=18 comparisons (**C**).

coefficient, balanced profiles considerably reduced negative modeled biomechanical outcomes both when balancing one and ten metrics, producing modeled outcomes significantly greater than zero ($p < 0.05$ and $p < 0.001$, respectively, one-sample Wilcoxon signed-rank test), with corresponding lower quartile normalized modeled metric outcomes of 0.05 and −0.01, respectively. This is a considerable improvement over preference-optimal profiles, which produced lower quartile modeled outcomes of −0.62 and −0.43 for the one- and ten-metric cases, respectively. Generally, maximizing modeled biomechanical metric outcomes led to poor modeled preference outcomes, and vice versa, corroborating results of individual biomechanical point metrics seen in Fig. 2 **B-D**.

An example of an individual patient's modeled biomechanical metric outcomes and preference outcomes for a balance of three biomechanical metrics with assistance preference is shown in Fig. 6. Metric-regularized preference maximization produced positive modeled outcomes for all three biomechanical metrics, corresponding to theoretical 7.4%, 6.8%, and 11.4% improvements relative to unassisted walking baseline values in peak hip abduction, peak ankle plantarflexion torque, and peak knee extension torque, respectively. This is in contrast to maximizing modeled preference in isolation, which yielded worse modeled outcomes of −7.5%, −4.5%, and −15.8% relative to unassisted walking baselines for the same biomechanical metrics. A similar effect was observed in modeled preference outcomes when comparing our method to methods that maximize modeled biomechanical outcomes in isolation. As seen in Fig. 6, all three biomechanical metric-optimal profiles yielded comparatively poorer preference outcomes than the balanced profile. The importance of tuning is also visible in Fig. 6, where the best and worst modeled biomechanical metric outcomes are shown for the same patient. The worst biomechanical metric outcomes corresponded to relative changes from unassisted walking of −21.2%, −12.5%, and −53.3% for peak hip abduction, peak ankle plantarflexion, and peak knee extension, respectively.

It became more difficult to find assistance parameter values that balanced modeled biomechanical and preference outcomes as more biomechanical metrics were considered. Fig. 5 **C** shows that reducing negative modeled metric outcomes via an increased penalization coefficient can greatly reduce corresponding modeled preference outcomes. For a penalization coefficient of $\alpha = 10^{0.5}$, normalized modeled preference outcomes from profiles that balanced ten metrics were significantly worse than those that balanced one metric ($p < 0.05$, two-sample Wilcoxon signed-rank test). Further investigation into this tradeoff revealed that negative modeled biomechanical responses are often specific to individual patients. Supplementary Fig. S3 shows the minimum penalization coefficient required to achieve positive modeled biomechanical outcomes when balancing an increasing number of metrics. The upper quartile patient (in terms of modeled biomechanical outcomes) required less penalization to achieve positive biomechanical outcomes and a greater number of metrics could be balanced than the lower quartile patient.

IV. Discussion

Preference-optimal assistance parameter values yielded significantly worse modeled biomechanical outcomes compared to metric optimal parameter values, such as for foot to floor angle at initial contact, propulsive impulse, and stance-swing ratio (see Fig. 2), and in some cases, even produced negative modeled biomechanical outcomes that could be theoretically harmful to a patient's rehabilitation. Similarly, metric-optimal assistance profiles led to poor corresponding

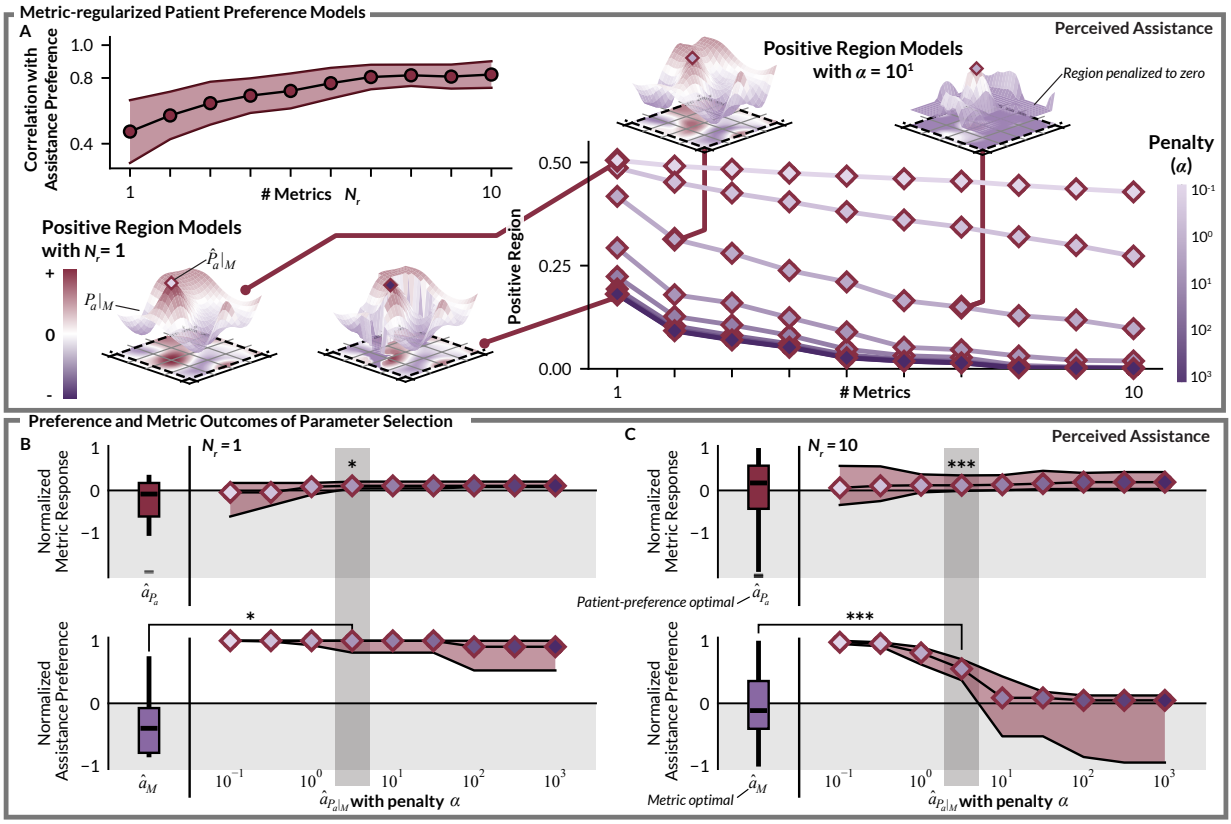

Fig. 5: Selecting optimal assistance parameter values that maximize modeled patient and clinician preference while ensuring positive modeled biomechanical outcomes. (**A**) Metric-regularized preference response landscapes that penalize negative modeled metric outcomes. Increasing the number of biomechanical metrics and penalization coefficient reduces the proportion of assistance parameter space that is positive. (**B, C**) Normalized modeled preference and metric outcomes from selecting assistance parameter values that maximize modeled metric ($\hat{M}$) or preference ($\hat{P}$) outcomes in isolation, and modeled metric-bounded preference outcomes with one metric (**B**) and ten metrics (**C**). Preference models were normalized to have zero mean and unit maximum value, and metric models were normalized such that zero corresponded to no change from unassisted walking, and to have unit maximum value. Normalized modeled metric outcomes significantly greater than zero assessed using a one-sample Wilcoxon signed-rank tests, shown at levels $^{*}p < 0.05$, $^{***}p < 0.001$. Normalized modeled perception outcomes significantly greater than $\hat{M}$ outcomes assessed using two-sample Wilcoxon signed-rank tests, shown at levels $^{*}p < 0.05$, $^{***}p < 0.001$.

modeled preference outcomes, with median modeled patient and clinician preference outcomes worse than the expected outcomes of selecting assistance profiles at random. This highlights limitations in existing methods of tuning assistive devices that either maximize biomechanics- or preference-based objective functions in isolation, and underscores the need for tuning methods for gait assistive devices that consider both biomechanical and preference outcomes together. Our findings align with previous studies in populations without neurological impairments that demonstrate a divergence between parameter values optimizing biomechanical or energetic outcomes, such as metabolic efficiency [26], [28], [29] and energy return [27], and those preferred by users, thereby extending this principle to post-stroke gait rehabilitation.

To examine the interplay between biomechanics and user preference, we developed a data-driven approach of identifying biomechanical determinants of modeled preference via an optimally weighted combination of models of biomechanical features extracted using MFPCA. Naturally, given a large enough set of extracted biomechanical features (96 from 12 variables) per participant, it is expected that patient and clinician preference models could be accurately approximated. It is surprising, however, that preference models could be approximated strongly ($\rho > 0.8$) with only three or four extracted biomechanical principal component models. There was a large amount of heterogeneity in the biomechanical variable types needed to approximate both patient and clinician preference responses; out of 12 variable types, no single variable consistently appeared in the top three variables used in patient or clinician approximations (see Supplementary Table S4).

To our knowledge, this study is the first to investigate the biomechanical determinants of preference in individuals with neurological gait impairments. It is known that these determinants are largely personal; prior works in populations without neurological impairments have been unable to resolve population-level determinants [29]. Combined with the inherently large heterogeneity in neurological impairments, it is unsurprising that there is large variability in determinants and low within-group preference correlations. Moreover, our cohort comprised of participants in the chronic phase of stroke recovery, and individuals across the recovery spectrum are likely to be even more heterogeneous.

More biomechanical feature models were needed to approximate modeled clinician safety preference than patient safety

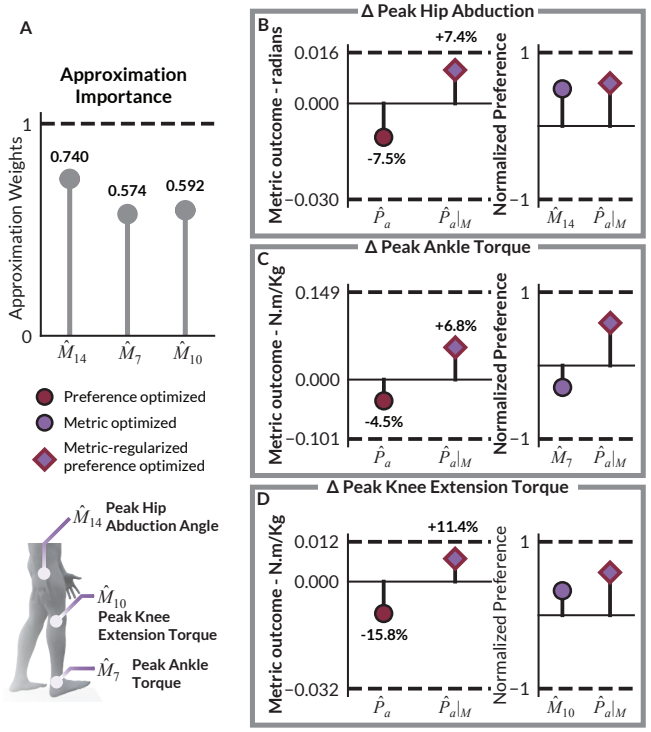

Fig. 6: Modeled outcomes of balanced tuning for an example patient. (**A**) The top three biomechanical point metrics important in approximating an individual patient's (P3) preference of assistance. (**B-D**) Modeled biomechanical point metric outcomes for peak hip abduction (**B**), peak ankle torque (**C**), and peak knee extension torque (**D**), and corresponding modeled preference outcomes when selecting assistance parameter values that maximize either modeled metric ($\hat{M}$) or preference ($\hat{P}$) outcomes in isolation, and metric-regularized preference ($\hat{P}_a|_M$). Dashed lines indicate best and worst modeled biomechanical metric and preference outcomes. Percentages above and below metric outcomes indicate % change from unassisted walking.

preference. This is expected, in part because the clinicians were not present during the patient walking trials, so preference may have been more complex to form based on video alone, but it also may also suggest that clinicians were considering a greater number of biomechanical features than patients were when forming their perception of safety. We further investigated groups of biomechanical variables that were important for approximating modeled preference, and found that anatomical location was a key factor. For clinicians, the pelvis was significantly important, potentially indicating that clinicians prioritized proximal kinematic changes occurring from the distal biomechanical changes propagating up the kinematic chain. For patients, the ankle appeared to be relatively important in approximating assistance preference, but less important in approximating safety preference; while the opposite was true for the knee (see Fig. 4 **C**). Knowing that a range of anatomical locations are important in approximating preference highlights the need for biomechanical monitoring across the body. We also found differences in kinematic versus kinetic variable approximation importance. Kinematic variables were significantly important in approximating clinician preference; this is expected, as visual information does not convey kinetic data. Surprisingly, kinetic variables were also not significantly important for patient preference, despite potential presumptions that these variables would be more prominently felt by a patient. Finally, while we found no relationship between whether a clinician had experience with FES and their preference response (see Supplementary Results S2. B.), further investigation is warranted to understand how a clinician's preference can be shaped by experience with gait-assistive devices.

Our method of metric-regularized preference maximization demonstrated the feasibility and benefits of balancing the multiple modeled biomechanical metric and user preference outcomes when tuning assistance parameter values. We used our method of approximating preference to obtain personalized sets of biomechanical metrics that are important in a patient's preference, and their relative weighting. Penalizing negative modeled biomechanical outcomes allowed us to regularize the preference response landscape used in assistance parameter tuning such that positive modeled outcomes were achieved in both domains. We found that balanced assistance profiles corresponded to significant improvements in modeled patient preference compared to metric-optimal profiles, and significantly positive modeled metric outcomes; something that was not the case for preference-optimal profiles. This confirms that our method was able to achieve its goal of maximizing modeled preference while ensuring lower bounds on modeled biomechanical outcomes were met.

While it was possible to balance multiple biomechanical metrics simultaneously, it became increasingly difficult to achieve for all patients with increasing numbers of biomechanical metrics, as stronger penalization was required to ensure that all modeled metric responses were positive (see Supplementary Fig. S3), which reduced the areas of the resultant response landscapes that produced favorable modeled preference outcomes (Fig. 5). The challenge in balancing multiple metrics at once lies in negative correlations between different biomechanical metrics, so improvements in certain metrics will result in reductions in others (see Supplementary Fig. S2). Maximizing modeled preference while using modeled biomechanical metric outcomes for regularization was favored, because biomechanical metric outcomes have a lower bound, so harmful outcomes could be penalized, while preference data has only directionality (due to its point-wise comparison format).

The benefits of balanced profiles that maximize preference while satisfying lower bounds on biomechanical metric outcomes are two-fold: first, from a behavioral perspective, maximizing patient and clinician preference reduces the likelihood of abandonment of the device. Second, from a biomechanical standpoint, satisfying lower bounds on biomechanical outcomes mitigates the risk harming a patient's gait, which can be damaging to their rehabilitation. An example of balancing three modeled biomechanical point metric outcomes with modeled patient assistance preference outcomes is shown for an example patient in Fig. 6. The balanced profile yielded positive modeled outcomes for both the three metrics (hip abduction angle, peak plantarflexion torque, knee extension torque) and normalized preference, compared to the preference-optimal (perceived assistance) profile, which resulted in negative modeled outcomes for all three metrics, and compared to the optimal profile for each

biomechanical metric, which resulted in comparatively reduced modeled preference outcomes. When considering the extremes of possible biomechanical metric outcomes, it is clear that poor tuning can lead to large negative consequences (see Fig. 6), corroborating our prior work [6] which showed that poor tuning could have a significant detrimental effect on biomechanical metric outcomes such as propulsion symmetry. Our approach of biomechanical metric-regularized preference maximization minimizes the risk of producing these negative outcomes, while increasing the likelihood of continued use.

Although this work provides a multi-perspective exploration of the relationship between biomechanics and preference, there are some limitations that should be considered for future research. As previously noted, the 2IFC and 2AFC paradigm for polling preference precludes the ability to compute a baseline for preference measures relative to a patient's or clinician's preference during unassisted walking. Clinician preference was collected from their assessment of patients' gait through recorded videos, rather than direct observation, and in isolation from patient preference responses. While this was intentional, to avoid confounding patient and clinician preference, this is not reflective of a typical tuning session for assistive devices, where patient-clinician discourse would enable a collaborative approach to tuning assistance. In terms of exposure, participants only compared each pair of assistance profiles once for a relatively short duration, and a follow up study was not conducted to verify the effects of balanced assistance. Further research will be needed to understand the longitudinal evolution of preference- and biomechanics-optimal assistance, as well as to quantify the outcomes of balanced assistance. Finally, our patient population of nine individuals post-stroke and single assistive device limit how well our findings can generalize to other populations and devices. Other neurological gait impairments, such as spinal cord injury, may lead to greater levels of impairment to perception, and other devices, such as exoskeletons, may be perceived differently than electrical stimulation. However, the work in this study can be used as a framework for understanding the impact of preference on biomechanics for other devices and populations.

We anticipate that our approach can be integrated into clinical practice and support personalized rehabilitation, however, we used specialized equipment such as motion capture and force plates to measure biomechanical outcomes. Advances in estimation methods that utilize wearable technology and non-specialized equipment, such as smartphones, could support the feasibility of implementing quantitative, individualized tuning strategies outside laboratory settings. Furthermore, we performed a grid search across assistance profiles to obtain complete biomechanics and preference datasets, but sample efficient human in the loop optimization techniques could be used to reduce computational complexity and tuning time when integrated into clinical practice.

V. Conclusion

In this work, we aim to address the disconnect between biomechanics and user preference in assistive device tuning, which can undermine both the effectiveness of assistance and long-term adherence. We show that selecting assistance parameter values to optimize either biomechanical or preference outcomes in isolation leads to poor outcomes in the other domain. We further demonstrate that complex preference outcomes can be reliably approximated using a small subset of biomechanical variables, offering insight into how an individual's biomechanics shape preference and highlighting the potential for preference estimation. Building on these findings, we proposed a framework that simultaneously combines biomechanical and preference outcomes to select a balanced assistance profile that results in positive preference and biomechanical outcomes.

The implications of this work extend beyond our current focus, with potential applications in rehabilitation contexts where biomechanical performance is prioritized while maintaining baseline levels of user satisfaction. We believe that integrating biomechanics and user preference will be crucial for wearable assistive technologies to achieve widespread clinical adoption and meaningfully improve rehabilitation outcomes.

Acknowledgment

The authors thank all participants in this study, A. Chin, T. Baker, G. Perlmutter, K. Baker, K. Garcia, and F. Kavassalis for their assistance facilitating the study, and P. Slade for feedback.

References

[1] A. Lakmazaheri, S. Song, B. B. Vuong, B. Biskner, D. M. Kado, and S. H. Collins, "Optimizing exoskeleton assistance to improve walking speed and energy economy for older adults," *Journal of NeuroEngineering and Rehabilitation*, vol. 21, no. 1, pp. 1–14, 12 2024.

[2] M. K. Ishmael, D. Archangeli, and T. Lenzi, "Powered hip exoskeleton improves walking economy in individuals with above-knee amputation," *Nature Medicine 2021 27:10*, vol. 27, no. 10, pp. 1783–1788, 10 2021.

[3] A. Esquenazi, M. Talaty, A. Packel, and M. Saulino, "The Rewalk powered exoskeleton to restore ambulatory function to individuals with thoracic-level motor-complete spinal cord injury," *American Journal of Physical Medicine and Rehabilitation*, vol. 91, no. 11, pp. 911–921, 11 2012.

[4] Z. F. Lerner, D. L. Damiano, and T. C. Bulea, "A lower-extremity exoskeleton improves knee extension in children with crouch gait from cerebral palsy," *Science Translational Medicine*, vol. 9, no. 404, 8 2017.

[5] L. N. Awad, J. Bae, K. O'Donnell, S. M. De Rossi, K. Hendron, L. H. Sloot *et al.*, "A soft robotic exosuit improves walking in patients after stroke," *Science Translational Medicine*, vol. 9, no. 400, 7 2017.

[6] D. K. Choe, A. J. Aiello, J. E. Spangler, C. J. Walsh, and L. N. Awad, "A Propulsion Neuroprosthesis Improves Overground Walking in Community-Dwelling Individuals After Stroke," *IEEE Open Journal of Engineering in Medicine and Biology*, pp. 1–10, 2024.

[7] F. Hussain, R. Goecke, and M. Mohammadian, "Exoskeleton robots for lower limb assistance: A review of materials, actuation, and manufacturing methods," *Proceedings of the Institution of Mechanical Engineers, Part H: Journal of Engineering in Medicine*, vol. 235, no. 12, pp. 1375–1385, 12 2021.

[8] T. M. Kesar, R. Perumal, D. S. Reisman, A. Jancosko, K. S. Rudolph, J. S. Higginson *et al.*, "Functional electrical stimulation of ankle plantarflexor and dorsiflexor muscles: Effects on poststroke gait," *Stroke*, vol. 40, no. 12, pp. 3821–3827, 12 2009.

[9] L. N. Awad, D. S. Reisman, R. T. Pohlig, and S. A. Binder-Macleod, "Reducing the Cost of Transport and Increasing Walking Distance after Stroke," *Neurorehabilitation and Neural Repair*, vol. 30, no. 7, pp. 661–670, 8 2016.

[10] D. G. Everaert, R. B. Stein, G. M. Abrams, A. W. Dromerick, G. E. Francisco, B. J. Hafner *et al.*, "Effect of a foot-drop stimulator and ankle-foot orthosis on walking performance after stroke: A multicenter randomized controlled trial," *Neurorehabilitation and Neural Repair*, vol. 27, no. 7, pp. 579–591, 9 2013.

[11] I. Safaz, H. Türk, E. Yaşar, R. Alaca, F. Tok, and I. Tuğcu, "Use and Abandonment Rates of Assistive Devices/Orthoses in Patients with Stroke," *Gulhane Medical Journal*, vol. 57, no. 2, pp. 142–144, 2015.

[12] B. Phillips and H. Zhao, "Predictors of Assistive Technology Abandonment," *Assistive Technology*, vol. 5, no. 1, pp. 36–45, 6 1993.

[13] C. M. Morrow, E. Johnson, K. N. Simpson, and N. J. Seo, "Determining factors that influence adoption of new post-stroke sensorimotor rehabilitation devices in the USA," *IEEE Transactions on Neural Systems and Rehabilitation Engineering*, vol. 29, pp. 1213–1222, 2021.

[14] J. Zhang, P. Fiers, K. A. Witte, R. W. Jackson, K. L. Poggensee, C. G. Atkeson *et al.*, "Human-in-the-loop optimization of exoskeleton assistance during walking," *Science*, vol. 356, no. 6344, pp. 1280–1283, 6 2017.

[15] Y. Ding, M. Kim, S. Kuindersma, and C. J. Walsh, "Human-in-the-loop optimization of hip assistance with a soft exosuit during walking," *Science Robotics*, vol. 3, no. 15, 2 2018.

[16] P. Slade, M. J. Kochenderfer, S. L. Delp, and S. H. Collins, "Personalizing exoskeleton assistance while walking in the real world," *Nature*, vol. 610, no. 7931, pp. 277–282, 10 2022.

[17] D. Park, J. An, D. Lee, I. Kang, and A. J. Young, "Human-in-the-loop Optimization of Hip Exoskeleton Assistance During Stair Climbing," *IEEE Transactions on Biomedical Engineering*, 2025.

[18] J. Wolff, C. Parker, J. Borisoff, W. B. Mortenson, and J. Mattie, "A survey of stakeholder perspectives on exoskeleton technology," *Journal of NeuroEngineering and Rehabilitation*, vol. 11, no. 1, pp. 1–10, 12 2014.

[19] S. M. Siedl and M. Mara, "What Drives Acceptance of Occupational Exoskeletons? Focus Group Insights from Workers in Food Retail and Corporate Logistics," *International Journal of Human–Computer Interaction*, vol. 39, no. 20, pp. 4080–4089, 12 2023.

[20] M. Tucker, E. Novoseller, C. Kann, Y. Sui, Y. Yue, J. W. Burdick *et al.*, "Preference-Based Learning for Exoskeleton Gait Optimization," *Proceedings - IEEE International Conference on Robotics and Automation*, pp. 2351–2357, 5 2020.

[21] K. A. Ingraham, C. D. Remy, and E. J. Rouse, "The role of user preference in the customized control of robotic exoskeletons," *Science Robotics*, vol. 7, no. 64, p. 3487, 3 2022.

[22] U. H. Lee, V. S. Shetty, P. W. Franks, J. Tan, G. Evangelopoulos, S. Ha *et al.*, "User preference optimization for control of ankle exoskeletons using sample efficient active learning," *Science Robotics*, vol. 8, no. 83, 10 2023.

[23] A. Alili, V. Nalam, M. Li, M. Liu, J. Feng, J. Si *et al.*, "A Novel Framework to Facilitate User Preferred Tuning for a Robotic Knee Prosthesis," *IEEE Transactions on Neural Systems and Rehabilitation Engineering*, vol. 31, pp. 895–903, 2023.

[24] J. M. Caputo, E. Dvorak, K. Shipley, M. A. Miknevich, P. G. Adamczyk, and S. H. Collins, "Robotic Emulation of Candidate Prosthetic Foot Designs May Enable Efficient, Evidence-Based, and Individualized Prescriptions," *Journal of Prosthetics and Orthotics*, vol. 34, no. 4, pp. 202–212, 10 2022.

[25] K. A. Ingraham, M. Tucker, A. D. Ames, E. J. Rouse, and M. K. Shepherd, "Leveraging user preference in the design and evaluation of lower-limb exoskeletons and prostheses," *Current Opinion in Biomedical Engineering*, vol. 28, p. 100487, 12 2023.

[26] S. A. Antos, K. P. Kording, and K. E. Gordon, "Energy expenditure does not solely explain step length–width choices during walking," *Journal of Experimental Biology*, vol. 225, no. 6, 3 2022.

[27] M. K. Shepherd and E. J. Rouse, "Rethinking Energy Storage and Return in Prosthetic Feet: User Preferences Challenge Conventional Wisdom," *Proceedings of the IEEE RAS and EMBS International Conference on Biomedical Robotics and Biomechatronics*, pp. 192–197, 2024.

[28] A. J. Young, J. Foss, H. Gannon, and D. P. Ferris, "Influence of power delivery timing on the energetics and biomechanics of humans wearing a hip exoskeleton," *Frontiers in Bioengineering and Biotechnology*, vol. 5, no. MAR, p. 230967, 3 2017.

[29] T. R. Clites, M. K. Shepherd, K. A. Ingraham, L. Wontorcik, and E. J. Rouse, "Understanding patient preference in prosthetic ankle stiffness," *Journal of NeuroEngineering and Rehabilitation*, vol. 18, no. 1, pp. 1–16, 12 2021.

[30] R. L. Medrano, G. C. Thomas, and E. J. Rouse, "Can humans perceive the metabolic benefit provided by augmentative exoskeletons?" *Journal of NeuroEngineering and Rehabilitation*, vol. 19, no. 1, pp. 1–13, 12 2022.

[31] M. K. Shepherd and E. J. Rouse, "Comparing preference of ankle–foot stiffness in below-knee amputees and prosthetists," *Scientific Reports*, vol. 10, no. 1, pp. 1–8, 9 2020.

[32] V. L. Feigin, B. A. Stark, C. O. Johnson, G. A. Roth, C. Bisignano, G. G. Abady *et al.*, "Global, regional, and national burden of stroke and its risk factors, 1990-2019: A systematic analysis for the Global Burden of Disease Study 2019," *The Lancet Neurology*, vol. 20, no. 10, pp. 1–26, 10 2021.

[33] W. Ding, S. Hu, P. Wang, H. Kang, R. Peng, Y. Dong *et al.*, "Spinal Cord Injury: The Global Incidence, Prevalence, and Disability From the Global Burden of Disease Study 2019," *Spine*, vol. 47, no. 21, p. 1532, 11 2022.

[34] E. Nichols, J. D. Steinmetz, S. E. Vollset, K. Fukutaki, J. Chalek, F. Abd-Allah *et al.*, "Estimation of the global prevalence of dementia in 2019 and forecasted prevalence in 2050: an analysis for the Global Burden of Disease Study 2019," *The Lancet Public Health*, vol. 7, no. 2, pp. e105–e125, 2 2022.

[35] P. Mahlknecht, S. Kiechl, B. R. Bloem, J. Willeit, C. Scherfler, A. Gasperi *et al.*, "Prevalence and Burden of Gait Disorders in Elderly Men and Women Aged 60–97 Years: A Population-Based Study," *PLOS ONE*, vol. 8, no. 7, p. e69627, 7 2013.

[36] C. K. Balasubramanian, R. R. Neptune, and S. A. Kautz, "Variability in spatiotemporal step characteristics and its relationship to walking performance post-stroke," *Gait & posture*, vol. 29, no. 3, pp. 408–414, 4 2009.

[37] L. Séléna, M. Betschart, R. Aissaoui, and S. Nadeau, "Understanding Spatial and Temporal Gait Asymmetries in Individuals Post Stroke," *American Journal of Physical Medicine & Rehabilitation*, vol. 2, no. 3, 3 2014.

[38] Y. Nishi, K. Ikuno, Y. Takamura, Y. Minamikawa, and S. Morioka, "Modeling the Heterogeneity of Post-Stroke Gait Control in Free-Living Environments Using a Personalized Causal Network," *IEEE transactions on neural systems and rehabilitation engineering : a publication of the IEEE Engineering in Medicine and Biology Society*, vol. 32, 2024.

[39] V. Kuptniratsaikul, A. Kovindha, S. Suethanapornkul, P. Massakulpan, W. Permsirivanich, and P. S. a. Kuptniratsaikul, "Motor recovery of stroke patients after rehabilitation: one-year follow-up study," *International Journal of Neuroscience*, vol. 127, no. 1, pp. 37–43, 1 2017.

[40] J. W. Chow and D. S. Stokic, "Longitudinal Changes in Temporospatial Gait Characteristics during the First Year Post-Stroke," *Brain Sciences*, vol. 11, no. 12, p. 1648, 12 2021.

[41] T. Sugavanam, G. Mead, C. Bulley, M. Donaghy, and F. Van Wijck, "The effects and experiences of goal setting in stroke rehabilitation – a systematic review," *Disability and Rehabilitation*, vol. 35, no. 3, pp. 177–190, 2013.

[42] M. Maier, B. R. Ballester, and P. F. Verschure, "Principles of Neurorehabilitation After Stroke Based on Motor Learning and Brain Plasticity Mechanisms," *Frontiers in systems neuroscience*, vol. 13, 12 2019.

[43] L. R. Sheffler and J. Chae, "Neuromuscular electrical stimulation in neurorehabilitation," *Muscle & Nerve*, vol. 35, no. 5, pp. 562–590, 5 2007.

[44] M. J. Taylor, A. J. Ruys, C. Fornusek, M. Bijak, M. Russold, and A. E. Bauman, "Lessons from Vienna: stakeholder perceptions of functional electrical stimulation technology and a conceptual model for practice," *Disability and Rehabilitation: Assistive Technology*, vol. 15, no. 1, pp. 37–44, 11 2018.

[45] T. Hornby, D. Straube, C. Kinnaird, C. Holleran, A. Echauz, K. Rodriguez *et al.*, "Importance of Specificity, Amount, and Intensity of Locomotor Training to Improve Ambulatory Function in Patients Poststroke," *Topics in Stroke Rehabilitation*, vol. 18, no. 4, pp. 293–307, 1 2011.

[46] S. J. Harkema, J. Hillyer, M. Schmidt-Read, E. Ardolino, S. A. Sisto, and A. L. Behrman, "Locomotor Training: As a Treatment of Spinal Cord Injury and in the Progression of Neurologic Rehabilitation," *Archives of Physical Medicine and Rehabilitation*, vol. 93, no. 9, pp. 1588–1597, 9 2012.

[47] B. J. Hafner, J. E. Sanders, J. Czerniecki, and J. Fergason, "Energy storage and return prostheses: does patient perception correlate with biomechanical analysis?" *Clinical Biomechanics*, vol. 17, no. 5, pp. 325–344, 6 2002.

[48] M. K. Shepherd, A. F. Azocar, M. J. Major, and E. J. Rouse, "Amputee perception of prosthetic ankle stiffness during locomotion," *Journal of NeuroEngineering and Rehabilitation*, vol. 15, no. 1, pp. 1–10, 11 2018.

[49] V. S. Shetty, U. H. Lee, K. A. Ingraham, and E. J. Rouse, "A Data Driven Approach for Predicting Preferred Ankle Stiffness of a Quasi-Passive Prosthesis," *IEEE Robotics and Automation Letters*, vol. 7, no. 2, pp. 3467–3474, 4 2022.

[50] H. Y. Hsiao, B. A. Knarr, J. S. Higginson, and S. A. Binder-Macleod, "The relative contribution of ankle moment and trailing limb angle to propulsive force during gait," *Human Movement Science*, vol. 39, pp. 212–221, 2 2015.

[51] C. E. Rasmussen and C. K. I. Williams, "Gaussian Processes for Machine Learning," *Gaussian Processes for Machine Learning*, 11 2005.

[52] W. Chu and Z. Ghahramani, "Preference learning with Gaussian processes," *International Conference on Machine Learning (ICML)*, pp. 137–144, 2005.